A 3D forward stratigraphic model of aeolian dune evolution for prediction of lithofacies heterogeneity

Na Yan [a,*], Luca Colombera [b], Grace I.E. Cosgrove [a], Nigel P. Mountney [a]

[a] *Fluvial, Eolian & Shallow-Marine Research Group, School of Earth and Environment, University of Leeds, Leeds, LS2 9JT, United Kingdom*
[b] *Department of Earth and Environmental Sciences, Università di Pavia, Via Ferrata 1, 27100, Pavia, Italy*

ARTICLE INFO

ABSTRACT

Within aeolian systems, complex dune morphologies can develop due to the interplay of a variety of allogenic and autogenic controls. As a result, the preserved sedimentary record of aeolian dune deposits is highly varied, exhibiting an array of sedimentary architectures and facies heterogeneities. However, reconstructions of such aeolian sedimentary architectures are usually based on limited information from one-dimensional borehole data or two-dimensional outcropping successions; as such, it is challenging to predict three-dimensional architectures and the distribution of small-scale facies heterogeneities of aeolian sedimentary successions. To address this, a novel rule-based forward stratigraphic model, the Dune Architecture and Sediment Heterogeneity model (DASH), has been developed to reproduce three-dimensional sedimentary bodies, bounding surfaces and associated facies distributions formed by a wide range of dune morphologies and morphodynamic behaviours. The model generates architectural frameworks produced by dune and interdune migration and aggradation, based on a long-established modelling approach; it then applies a series of rules that reflect geological understanding or observations from geological analogues to populate the three-dimensional space with facies domains. The model has been applied to simulate the stratal architectures and facies organization of (i) three idealized examples of successions produced by different dune morphologies, and (ii) a real-world case example from the Triassic Helsby Sandstone Formation, Cheshire Basin, UK. The results demonstrate how the model can be used to predict likely facies distributions in three dimensions, which themselves can be used to constrain models of petrophysical properties constructed with geostatistical techniques. The model can therefore be applied to assist reconstructions of subsurface architectures and petrophysical heterogeneity.

1. Introduction

Aeolian sedimentary systems and their preserved successions develop complex sedimentary architectures due to their sensitivity to a wide range of environmental variables, including sediment supply, wind regime, water-table level, and vegetation cover (Fryberger, 1979; Lancaster, 1997; Wasson and Hyde, 1983; Yan and Baas, 2015). At a gross scale, packages of aeolian strata are sometimes regarded as lithologically homogeneous because their deposits are dominantly characterized by relatively well-sorted sand (Bagnold, 1941). Yet at the scale of bedsets, aeolian dune and interdune deposits typically contain significant facies heterogeneities (e.g., McKee, 1966; Romain, 2014), and these may determine variability in porosity and permeability, and thus affect fluid flow and solute transport in preserved successions (Mullins et al., 2022). In particular, the juxtaposition of dune and interdune deposits – for example due to the autogenic migration and climb of a train of dunes with intervening interdune flats, else in relation to spatial or temporal fluctuations in water-table level – can lead to significant variability in the composition and grain size of accumulated sediments. This gives rise to heterogeneity in lithology, and porosity and permeability heterogeneity and anisotropy (Al-Masrahy, 2020; Kocurek, 1981; Mountney and Thompson, 2002).

Aeolian systems can develop a varied range of sedimentary architectures and facies arrangements, resulting from the interplay of both allogenic and autogenic controls (Mountney, 2006; Rubin and Carter, 2006). As a result, internal sedimentary architectures and facies distributions in accumulated sedimentary successions of dune and interdune systems can be very complex and difficult to predict (Rodríguez-López et al., 2014). Most reconstructions of aeolian sedimentary architectures are based on information available from either one-dimensional

* Corresponding author.
E-mail address: n.yan@leeds.ac.uk (N. Yan).

datasets, such as from cores and well logs (e.g., Lindquist, 1988; Luthi and Banavar, 1988; North and Boering, 1999; Romain and Mountney, 2014), or from two-dimensional outcropping successions (e.g., Glennie and Provan, 1990; Kocurek et al., 1991; Gross et al., 2023). Other reconstructions of aeolian sedimentary architectures are based on numerical modelling approaches. Rubin (1987) and Rubin and Carter (2006) developed a modelling tool for the simulation of the three-dimensional stratigraphic architectures of cross-strata and related bounding surfaces by means of a deterministic geometric approach. However, this model cannot be readily employed to reconstruct the possible internal facies distributions of aeolian successions. Mountney (2012) developed a two-dimensional model to simulate the accumulation of aeolian deposits in relation to spatio-temporal variations in the size and spacing of dunes, their migration rate, and the aggradation rate, but only a limited number of basic types of behaviour are examined, and internal facies variations within individual dunes and interdunes are not considered.

The complexity of dune dynamics gives rise to a highly varied range of dune and interdune morphologies (e.g., barchan dunes, transverse dunes, longitudinal dunes, compound and complex dunes – *sensu* McKee and Bigarella, 1979), and dry, damp and wet interdunes (e.g., Kocurek et al., 1991; Kocurek and Havholm, 1993; García-Hidalgo et al., 2002). An array of depositional processes operate on different parts of dunes and interdunes, and these lead to the accumulation of complex arrangements of lithofacies units (Mountney, 2006). Therefore, it remains challenging to predict the three-dimensional sedimentary architecture and small-scale facies distributions within aeolian successions.

This article presents a novel rule-based forward stratigraphic model: the Dune Architecture and Sediment Heterogeneity model (DASH). This new model is based in part on the earlier geometric model by Rubin (1987) and Rubin and Carter (2006), but additionally enables the three-dimensional distribution of domains with different types of sedimentary facies to be predicted. The aim is to demonstrate how the new model can be applied as a tool for the prediction of internal sedimentary architectures in three dimensions in a way that allows prediction of likely facies distributions and resulting petrophysical heterogeneity. Specific objectives are as follows: (i) to compare sedimentary architecture and facies distribution of common dune types that are widespread in aeolian sand seas (ergs) globally, using simplified and idealized examples (transverse dunes and longitudinal dunes), and compound superimposed dunes; (ii) to demonstrate how the migration of different dune types results in markedly different petrophysical heterogeneities in resultant deposits; and (iii) to illustrate how the model can be used to assist in gaining improved understanding of facies distributions and petrophysical properties of aeolian successions produced by different aeolian dune geomorphologies and geological histories.

2. Modelling algorithm

The DASH model is a geometric, rule-based forward stratigraphic model that builds upon the approach used by Rubin (1987) and Rubin and Carter (2006) to produce different hierarchies of internal architectures and bounding surfaces of aeolian deposits. However, the DASH model is novel in that it significantly enhances this earlier work by applying a rule-based approach to predict and model three-dimensional (3D) distributions of facies units within architectural elements for many different types of aeolian system. The DASH model incorporates rules of facies organization based on observations from many natural systems. These rules can be specified based on data from geological analogues, for example using sedimentological data extracted from the Database of Aeolian Sedimentary Architecture (DASA; Cosgrove et al., 2021). The DASH model is vector-based and written in Matlab. It can run simulations as a batch process using input files of pre-defined parameters.

The DASH model simulates stratigraphic architectures (stratal packages and associated bounding surfaces) produced by migrating aeolian bedforms and their accumulated successions using the
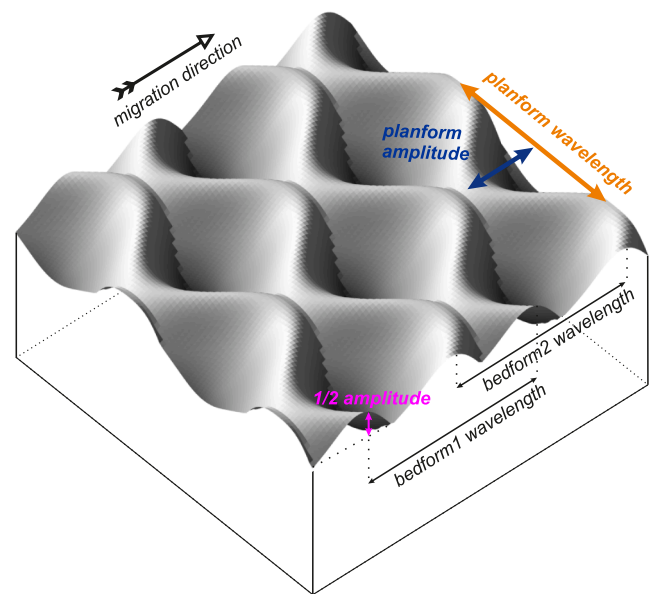
Fig. 1. Definition of some of the inputs to the modelling algorithm. Two sets of bedforms are used to create transverse dunes with out-of-phase crestlines. Curved crestlines are also simulated with a sine function defined by its wavelength and amplitude. No scale intended.

deterministic geometric approach developed by Rubin (1987) and Rubin and Carter (2006). The open-source Matlab code Bedforms 4.0 of Rubin and Carter (2006) can be downloaded from the website of the U.S. Geological Survey (Rubin and Carter, 2005). In the DASH model – as in the Bedforms 4.0 model of Rubin and Carter (2006) – bedform morphologies are modelled using modified sine curves (Fig. 1). Displacement of these sine curves over a series of time steps and in 3D mimics the migration behaviour of many naturally occurring dune types. The direction of bedform displacement can be specified in the modelling domain. The rate of displacement (in non-dimensional or predefined horizontal unit per iteration) is also controlled by a sine curve defined by its mean value, amplitude, period, and phase. The rate of displacement is constant through time when the amplitude is set to 0. The asymmetry of dunes (stoss slope vs. lee slope) can be adjusted by changing the relative phase of two sinusoidal components with different wavelengths, i.e., the bedform wavelength and one-half of bedform wavelength, respectively. The dune height is controlled by the amplitude of the sine curves. Variations in dune height relative to bedform wavelength generate bedforms of different steepness. Both the asymmetry and steepness of the bedforms can also vary with time according to sinusoidal functions. The plan-form morphology of dunes can be specified by means of one or two sinusoidal curves. Each curve can vary in wavelength, amplitude, phase, and migration speed perpendicular to the dune migration direction. Crescent-shaped bedforms can be generated by setting the wavelength of the first curve as twice that of the second one. These parameters determine one set of bedforms. They can be combined with two additional sets of bedforms in different ways (e.g., simple addition, proportional change, and local highest) to simulate compound and complex dunes (*sensu* McKee, 1979) with superimposed bedforms. As such, geometrically complicated stratal sets and their bounding surfaces may be generated – see Rubin (1987) for a fuller explanation of the original model.

The novelty of DASH lies in its ability to model the internal distributions of domains with distinct facies characteristics within larger-scale dune and interdune architectural elements. Facies domains are modelled in 3D using a series of rule sets that consider the geometry, distribution and topology of fundamental lithological types within the model. Principal amongst these rules are (i) the inclination of the surface slope, and (ii) the position along the depositional profile of a dune or
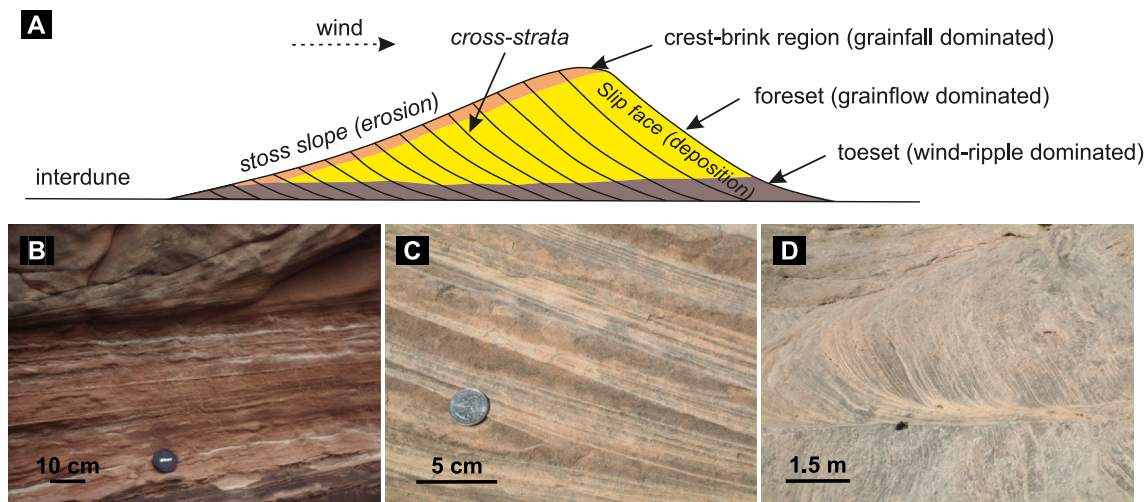
Fig. 2. (A) Dune morphology, internal stratal geometries and example facies domains seen in cross-section. No scale intended. Grainfall deposits dominate at the brink of the dune slipface. Grainflow deposits accumulate on dune lee slopes (slipfaces) at the angle of repose (30–34° for non-compacted, dry sand). Intercalated grainfall and grainflow strata can develop between the dune brink and upper foreset. Wind-ripple deposits accumulate on low-angle-inclined dune plinths and interdune areas. Between the foreset and toeset, packages of intercalated wind ripple and grainflow strata form. The direction of dune migration is from left to right in the section. (B) Damp-interdune wavy-laminated facies overlain by wind-ripple strata and grainflow at dune toe regions. Triassic Helsby Sandstone Formation, UK. (C) and (D) Intercalated grainflow (darker) and wind-ripple (paler) facies in dune plinth regions. Permian Cedar Mesa Sandstone, Utah, USA.

interdune. In combination, these variables are closely associated with different facies types observed in nature. These rules are employed to map in three dimensions the preserved expression of different depositional domains characterized by contrasting facies make-ups. These rules are established in a way that reflects our understanding of the distributions of sediments and smaller-scale bedforms on modern dunes, and the corresponding distributions of lithofacies in ancient aeolian successions; these rules are defined by the user, and can be changed to match quantifications of outcrop successions (Cosgrove et al., 2021). The application of these rules enables a detailed reconstruction of the distribution of domains characterized by differences in the likelihood of occurrence of certain lithofacies types. For example, the lithologies of dune successions are related to variations in the dominance of different processes across physiographic domains of dune and interdune environments (Al-Masrahy and Mountney, 2013; Mountney, 2006; Reading, 2009, Fig. 2). Grainfall deposits comprise sand entrained by the wind in suspension and typically deposited beyond the brink of the dune slipface due to flow separation (Kocurek and Dott, 1981). However, homogeneous packages of grainfall facies (very-fine sand) are not commonly preserved in ancient dune successions since they are mostly reworked as dune migration proceeds. As sand in saltation from the windward slope accumulates near the dune brink, avalanching occurs as grainflows down a lee-slope slipface inclined at the angle of repose (Hunter, 1977). Tongues of well-sorted and loosely packed grainflow deposits, many of fine-medium sand, commonly extend down to the lower part (plinth) of the lee slope (Inman et al., 1966; Yaalon and Laronne, 1971). Wind ripples develop by sand creep and saltation, and their strata comprise interlaminated silt, very fine to fine sand (Kocurek et al., 1999). Wind-ripple facies typically occur on the stoss slopes of barchan or transverse dunes, else on dune plinths inclined at less than 15°, and within or near flat-lying interdune areas. The size and shape of interdune regions are controlled by dune morphology, size, spacing and temporal variations thereof (Al-Masrahy and Mountney, 2013). Interdune deposits can develop under dry, damp or wet conditions (Kocurek and Dott, 1981). Dry interdune deposits may be dominated by wind-ripple facies, whereas water-table influenced damp or wet interdune deposits may be dominated by adhesion strata, precipitates or subaqueous deposits (Kocurek and Dott, 1981; Mountney and Russell, 2006).

Based on these predictable characteristics, facies domains that reflect physiographic depositional niches are determined on any two-dimensional (2D) vertical or horizontal sections of a 3D volume for which preserved stratal geometries have been modelled; this is accomplished within the DASH model using the following: (i) the true dip of strata (δ), which is calculated as:

$$\tan \delta = \frac{\tan \alpha}{\sin \beta} \qquad (1)$$

where α is the apparent dip and β is the angle between strike and apparent dip direction, both of which can be acquired from the modelled horizontal slices and cross sections of the strata; and (ii) the local convexity of the stratal surface (i.e., concave-upward vs. convex-upward shape) to differentiate upper and lower parts of dune foresets with similar dip angles. The extent of the facies domains for each simulation can be defined as a user-determined input based on threshold values of the physiographic variables. The default settings include six domains, which are adequate to represent the facies complexity most often observed in nature. From the lower to the higher parts of the formative aeolian topography, these default facies domains are as follows: (i) interdune-flat deposits, $\delta = 0°$; (ii) lower dune plinth deposits, which may typically comprise of reworked wind-rippled sandstone, $0° < \delta \leq 8°$; (iii) upper dune plinth deposits, which may be characterized typically by intercalated wind-ripple and grainflow strata, $8° < \delta \leq 16°$; (iv) lower foreset strata, which may be dominated by interbedded grainflow-grainfall deposits $16° < \delta \leq 25°$; (v) middle foreset strata, typically dominated by grainflow facies on the slipface, $\delta > 25°$; and (vi) deposits of the dune crest-brink to upper foreset region, characterized by slightly convex-upward accretion surfaces and $0° < \delta \leq 25°$, which may be dominated by grainfall strata beyond the brink point and by wind-ripple strata on the dune stoss side, if and where preserved. The geometry of interdune deposits and the angle of climb are determined by the temporal variations in dune height, migration speed, and deposition rate, which can be defined by either a function or a list. Being able to set the value for these parameters from a series of entries in lists of temporal variations provides flexibility to match modelled outcomes to real-world cases. Moreover, spatial resolutions can be customized to be smaller than unity. Sets of closely spaced 2D sections act as numerical descriptions of internal sedimentary architectures. These modelled pseudo-3D sedimentary architectures can be exported as fully 3D Cartesian geocellular grids, as ASCII or GSLib (Deutsch and Journel, 1992) files, in which the facies domains are coded as categorical variables.
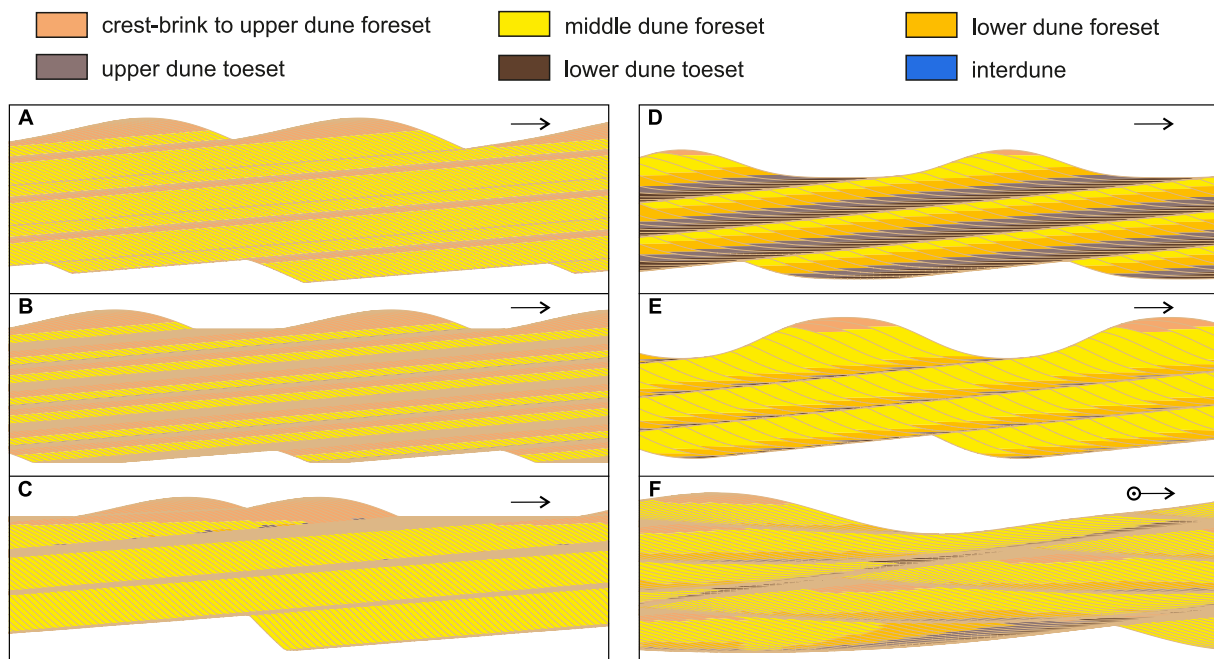
Fig. 3. Examples of modelled cross sections by DASH. Default facies-domain types are used. No scale intended. Black arrows show dominant wind directions. The cases from A to E are dominantly controlled by unidirectional wind, whereas the case F is controlled by two dominant wind directions that are perpendicular to each other, i.e., one wind direction to the right and another wind direction out of the page. (A) A cross section of the stratigraphy produced by transverse dunes without interdune flat. (B) A cross section of the stratigraphy produced by transverse dunes with interdune flat. Dunes maintain the same size while migrating towards the dominant wind direction. (C) A cross section of the stratigraphy produced by transverse dunes with interdune flat. Dunes decrease in height while migrating. A-C are generated with out-of-phase sinuous crestlines. (D) A cross section of the stratigraphy produced by linear dunes close to the sinuous crestlines. (E) A cross section of the stratigraphy produced by linear dunes further away from the sinuous crestlines. D and E are generated by perfectly longitudinal bedforms with along-crest migrating sinuosity. (F) A cross section of the stratigraphy produced by more complicated bedforms with along-crest migrating superimposed bedforms.

Examples of modelled cross sections are shown in Fig. 3, in which the default facies-domain types are used.

Inputs to the DASH model can be obtained from DASA, a relational database that stores data on the facies organization and sedimentary architecture of many known natural examples of aeolian systems and their preserved successions (Cosgrove et al., 2021). Currently, standardized data from 87 literature case studies of ancient aeolian systems and their preserved successions are contained in DASA. A case study is associated with one or more sets of data, termed 'subsets' (cf.Colombera et al., 2012); these are classified collections of data from which quantitative metrics can be extracted. Quantitative outputs can be retrieved from DASA on geological entities (e.g., facies units) at multiple scales, including outputs on their type, geometry, spatial relations, hierarchical relations, temporal significance, and textural and petrophysical properties. Associated metadata (e.g., basin setting, aeolian physiographic setting, geological age) are also stored (Cosgrove et al., 2021). DASA records the containment of smaller-scale elements within higher-order elements; for example, a subset (e.g., published graphic sedimentary log) can contain various architectural elements (e.g., an aeolian dune or interdune), which in turn can contain various lithofacies units within it (e.g., packages of grainflow or wind-ripple strata). These, in turn, may be associated with specific geological or petrophysical properties (e.g., values of porosity and permeability). DASA can be queried to provide quantitative metrics describing the spatial and hierarchical arrangement of lithofacies, and their geometric properties (e.g., thickness, length and width) from real-world examples, which can then be used to devise rules in the DASH model to constrain facies domains.

3. Applications to geocellular modelling

The grids produced by the DASH model are coded according to a categorical variable that specifies the facies domains reflecting the physiographic portions of the aeolian system being modelled (e.g.,

interdune, dune toeset, dune foreset). In each model output, the distribution of these categorical variables is deterministic. However, these grids can be subsequently used for obtaining stochastic models of facies or petrophysical heterogeneity, in different ways.

For example, if a geocellular grid containing facies of specified proportions is desired, this can be obtained using the domains as regions that can subsequently be populated with different 'facies' classes (which may be convenient groups of lithofacies) using pixel-based geostatistical modelling algorithms, such as Sequential Indicator Simulations (Deutsch and Journel, 1992). These modelling regions could each be characterized by different probabilities of occurrence of the different facies types, which would be expressed as auxiliary variables in the geocellular modelling step (cf. Colombera et al., 2018). If instead the facies domains approximate the facies categories that may need to be modelled (e.g., slipface, dune plinth), their proportions may be readily adjusted using tools that are commonly employed for this purpose in geocellular modelling practice (Journel and Xu, 1994; Remy et al., 2009). The outputs of the DASH model cannot be conditioned to directly honour local observations, such as borehole data; however, the resulting grids can be employed as training images for constraining subsurface models based on multipoint statistics (Strebelle, 2002), for which well conditioning is possible.

Alternatively, in a context where the reconstruction of likely porosity and/or permeability fields is required, it may be possible to skip the intermediate facies-modelling step by using the facies domains to directly model the distribution of petrophysical properties inside them. This can be done based on knowledge of both the likelihood of finding certain facies types in a given domain and of the expected distribution of the property of interest (porosity, permeability, etc.) of each facies type, which is typically based on observations from real-world examples. Specifically, DASA outputs on petrophysical properties of lithofacies (e. g., grainflow or wind-ripple strata) from geological analogues can be employed to this end. The distribution of petrophysical properties in the
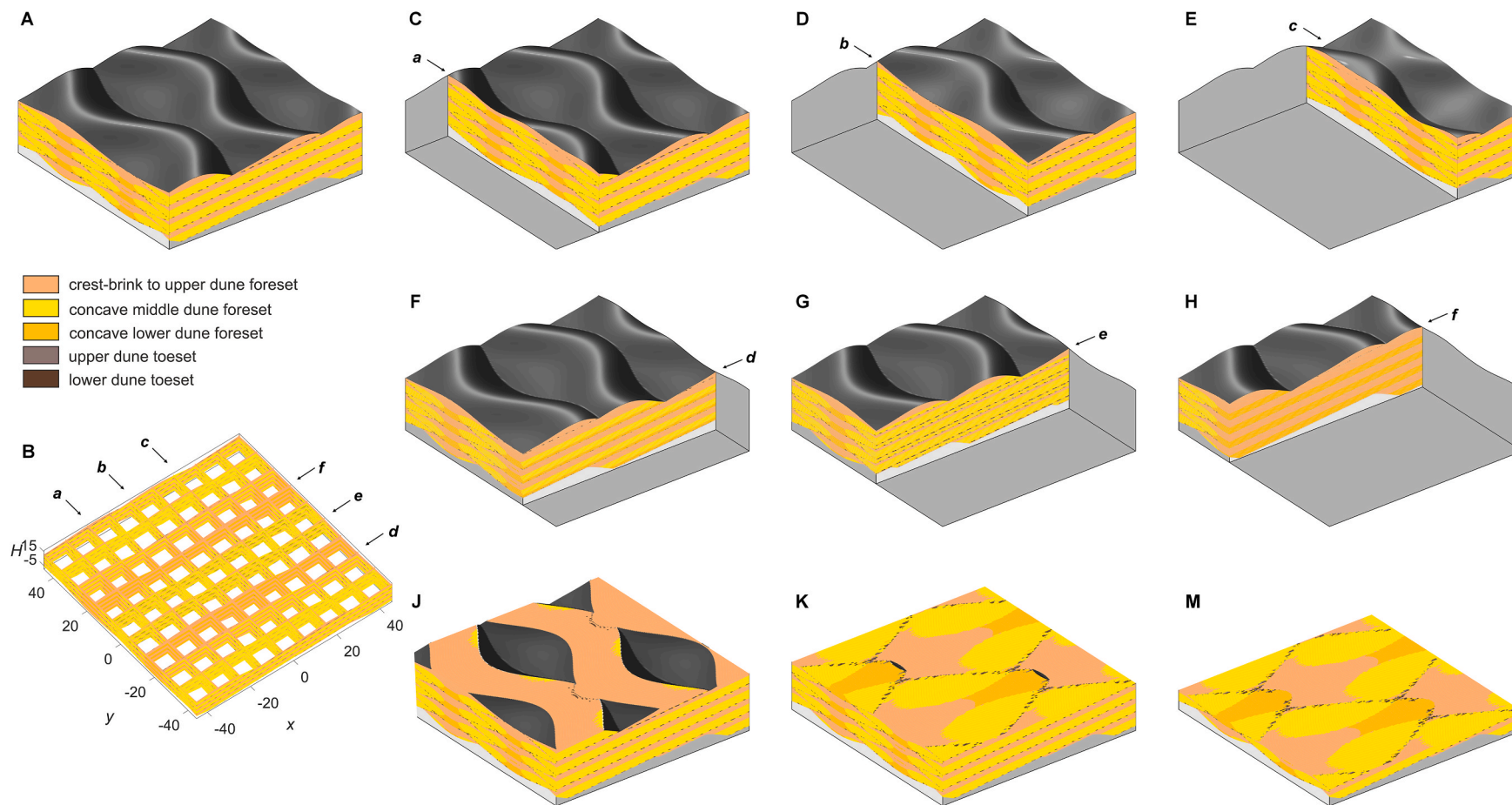
Fig. 4. Three-dimensional geomorphology and sedimentary architecture and lithofacies distributions typical of transverse bedforms with sinuous, out-of-phase crestlines. Parameters are the same as the Case 34a in Rubin and Carter (2006). Default facies domains are used. No scale intended.
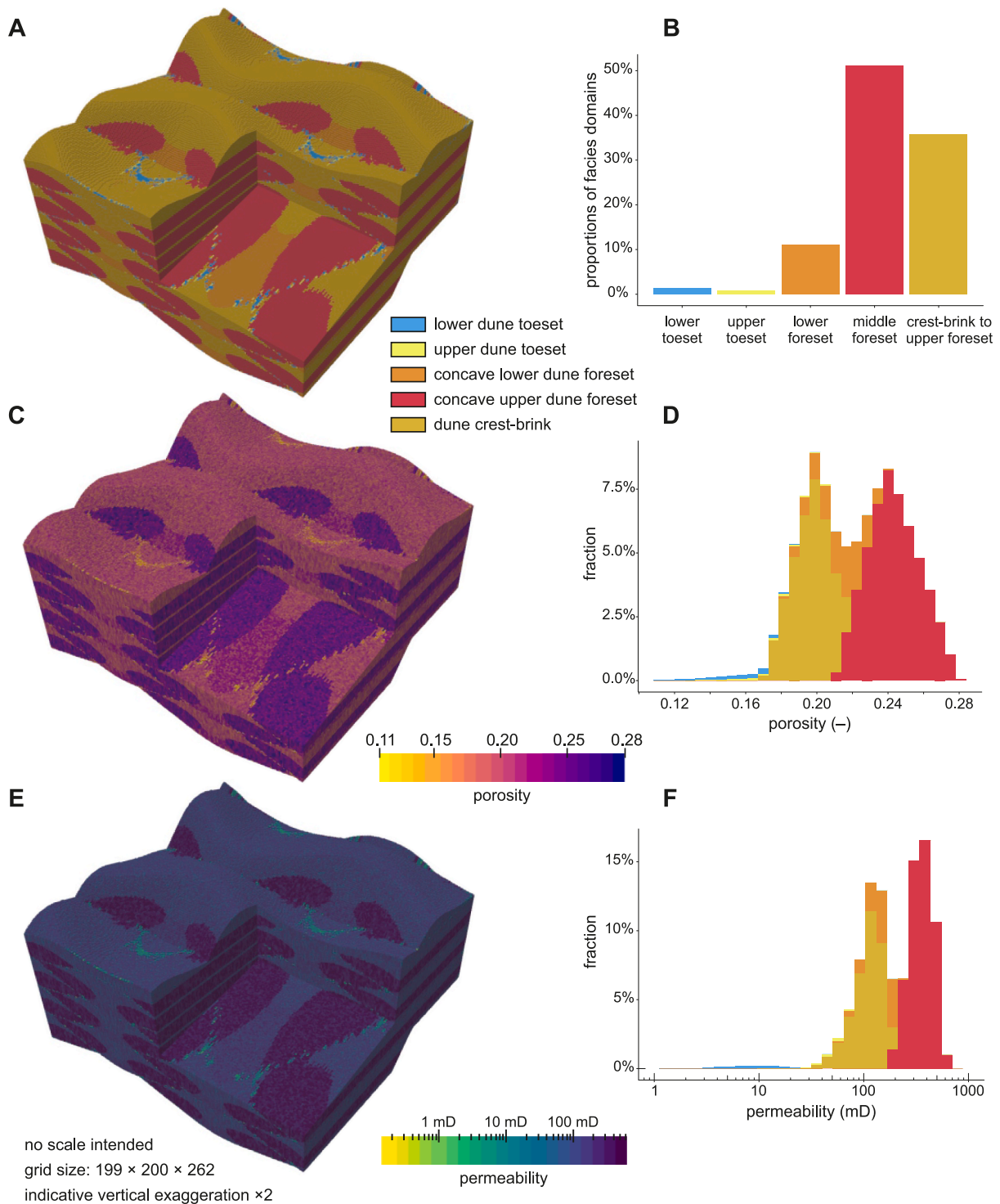
Fig. 5. Outputs of static geocellular modelling informed by DASH, for a succession related to transverse dunes with sinuous out-of-phase crestlines. (A) Geocellular model of DASH facies domains, with their proportions charted in (B). Facies-domain proportions reflect in part the full preservation of modelled bedforms on the top surface: the proportion of crest-brink to upper foreset domain volumes is ca. 29% in the part of grid underlying the top surface, as opposed to ca. 36% in the entire grid. (C) Realization of a Sequential Gaussian Simulation of porosity values modelled in the facies domains shown in (A); distributions of porosity values vary across the facies domains as shown in (D). (E) Realization of a Sequential Gaussian Simulation of permeability values modelled in the facies domains shown in (A); distributions of porosity values vary across the facies domains as shown in (F). Note that in the majority of ancient successions, the original dune topography and the facies associated with it are not preserved.

different facies domains can be modelled, for example, using Sequential Gaussian Simulations, applied jointly, or following a cookie-cut approach whereby properties are modelled independently for each facies domain and are then merged into a single grid (Remy et al., 2009).

Static property models generated in this way can be applied again as training images, or as reference models in subsurface studies that envisage flow-based upscaling (Nordahl et al., 2014). Examples of static models built with a cookie-cut modelling approach are shown below.
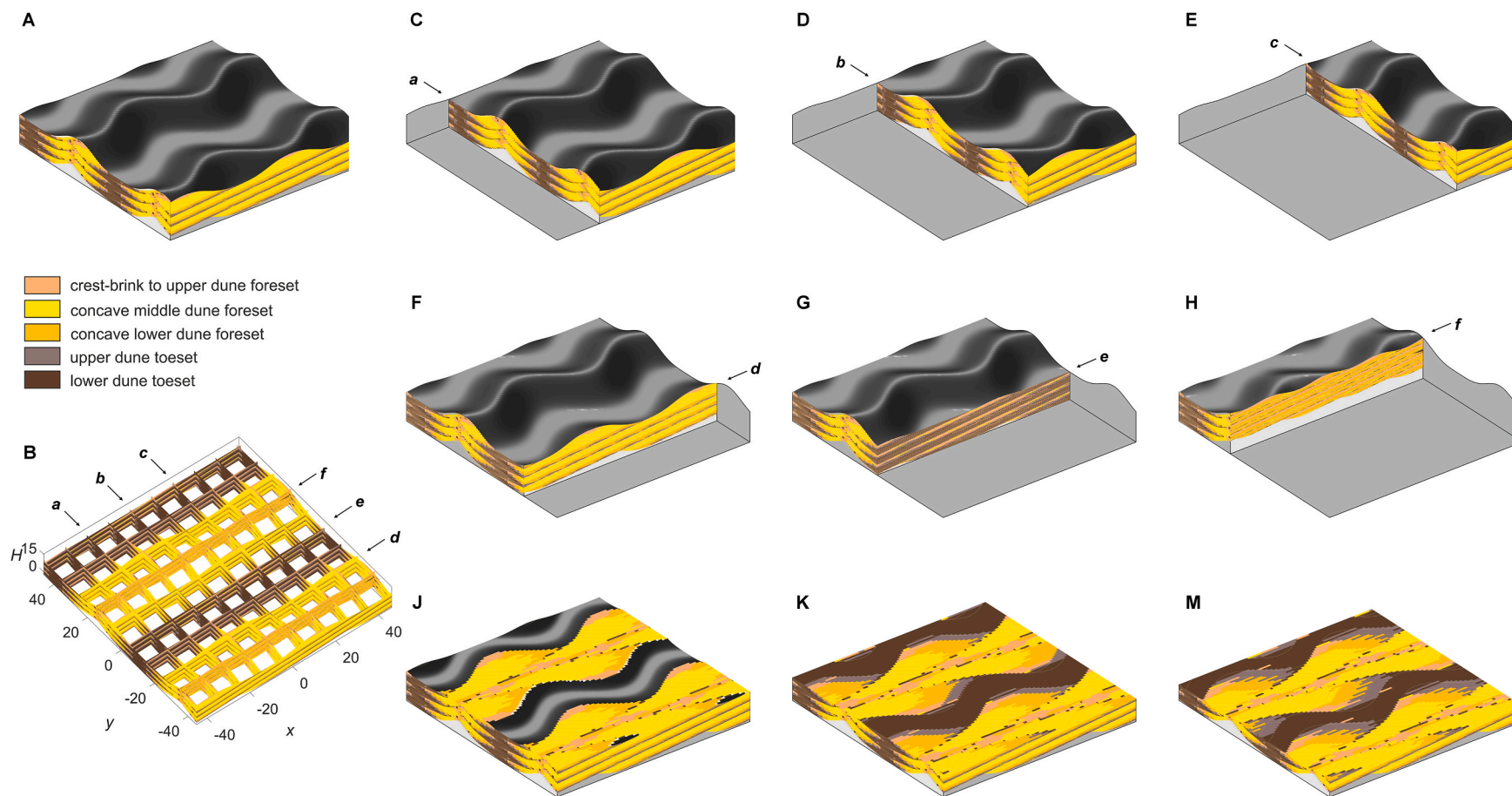
Fig. 6. Three-dimensional geomorphology and sedimentary architecture and lithofacies distributions of idealized longitudinal bedforms without net lateral migration. Parameters are the same as the Case 55 in Rubin and Carter (2006). Default facies domains are used. No scale intended.
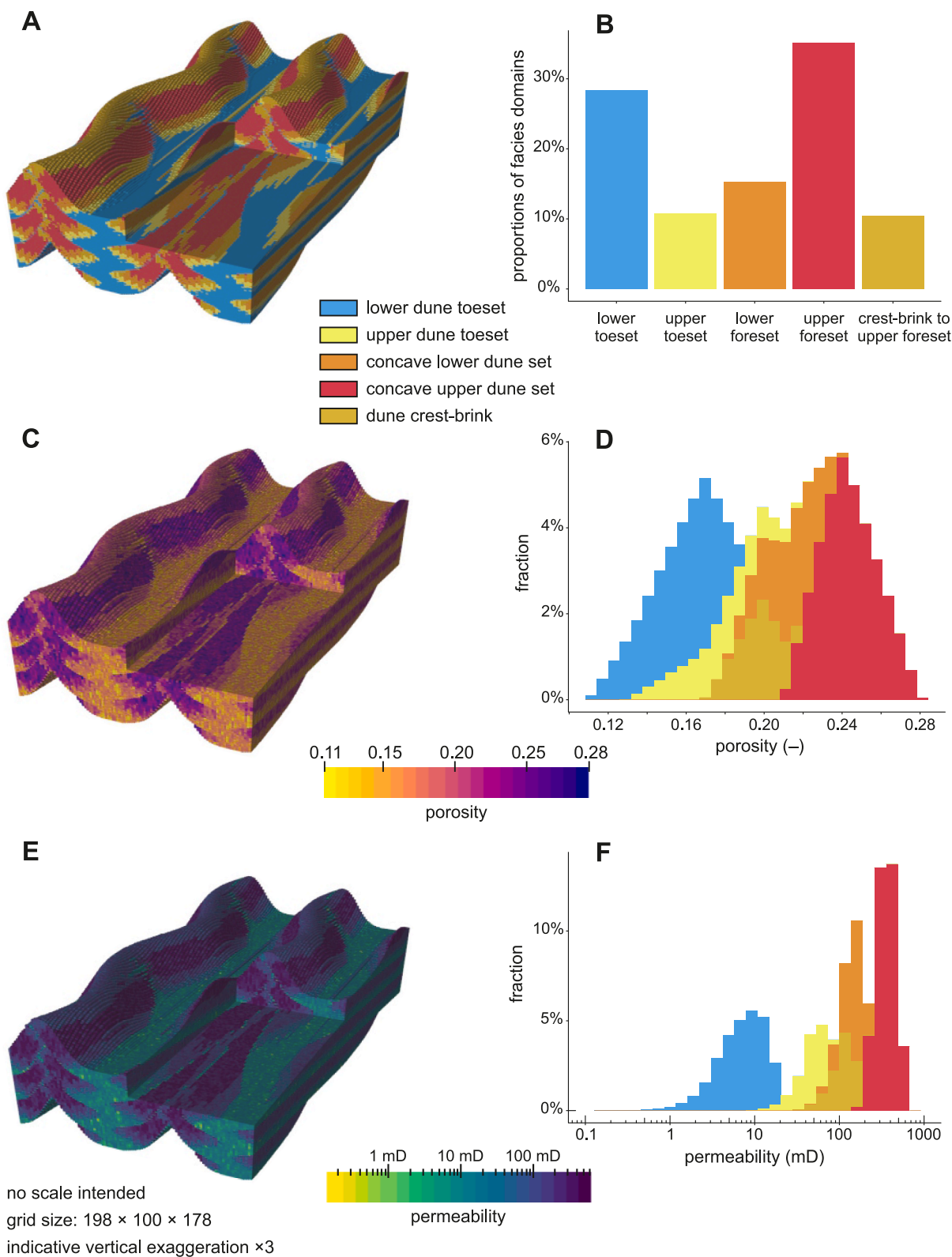
Fig. 7. Outputs of static geocellular modelling aided by DASH, for a succession related to sinuous linear dunes. (A) Geocellular model of DASH facies domains, with their proportions charted in (B). Facies-domain proportions reflect in part the full preservation of modelled bedforms on the top surface: the proportion of crest-brink to upper foreset domain volumes is ca. 7% in the part of grid underlying the top surface, as opposed to ca. 10% in the entire grid, whereas the proportion of lower-toeset strata is ca. 35% below the surface topography instead of ca. 28% as in the whole grid. (C) Realization of a Sequential Gaussian Simulation of porosity values modelled in the facies domains shown in (A); distributions of porosity values vary across the facies domains as shown in (D). (E) Realization of a Sequential Gaussian Simulation of permeability values modelled in the facies domains shown in (A); distributions of porosity values vary across the facies domains as shown in (F). Note that in the majority of ancient successions, the original dune topography and the facies associated with it are not preserved.
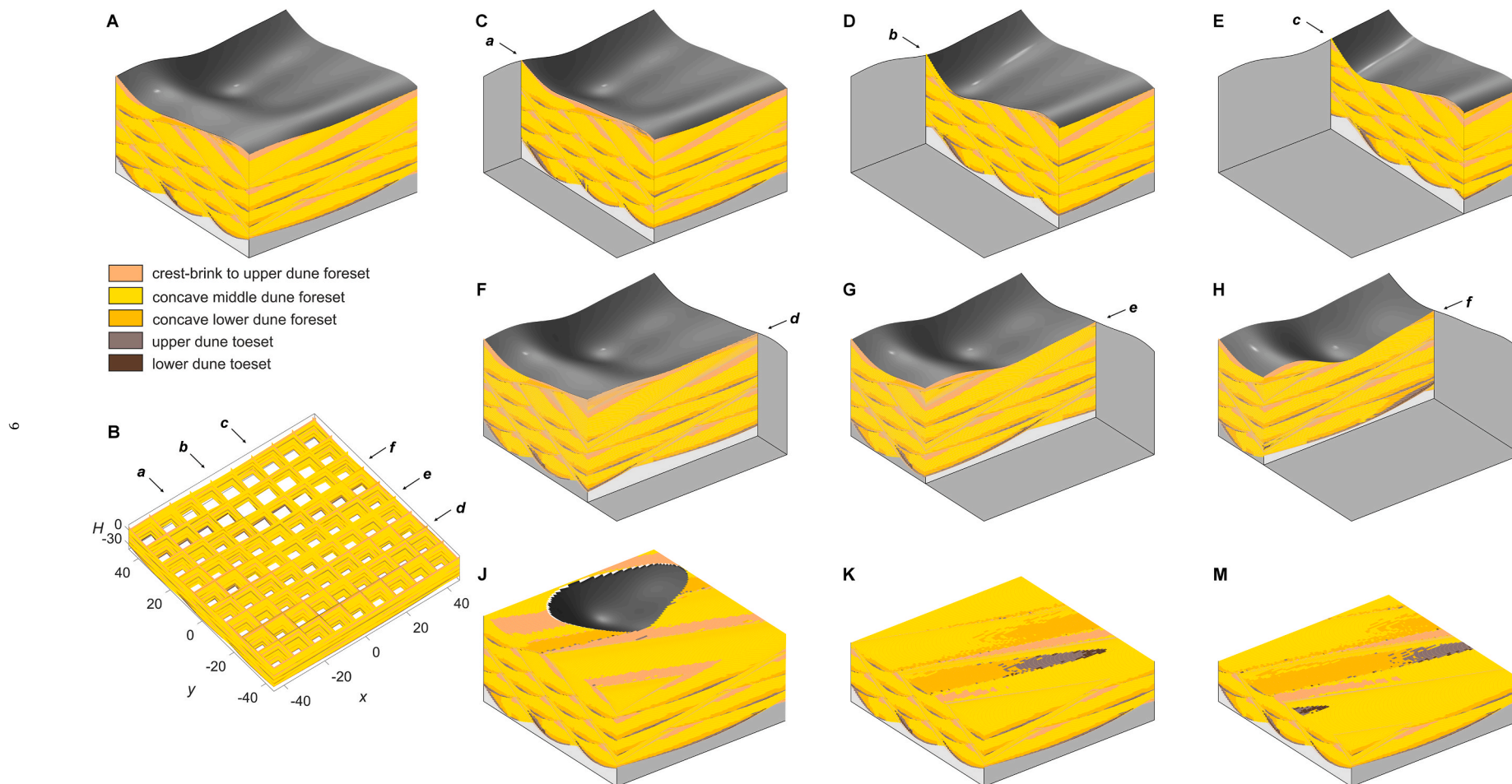
Fig. 8. Three-dimensional geomorphology and sedimentary architecture and lithofacies distributions of superimposed bedforms that undertake along-crest migration relative to the trend of the main (parent) bedforms. Parameters are the same as the Case 46l in Rubin and Carter (2006). Default facies types are used. No scale intended.
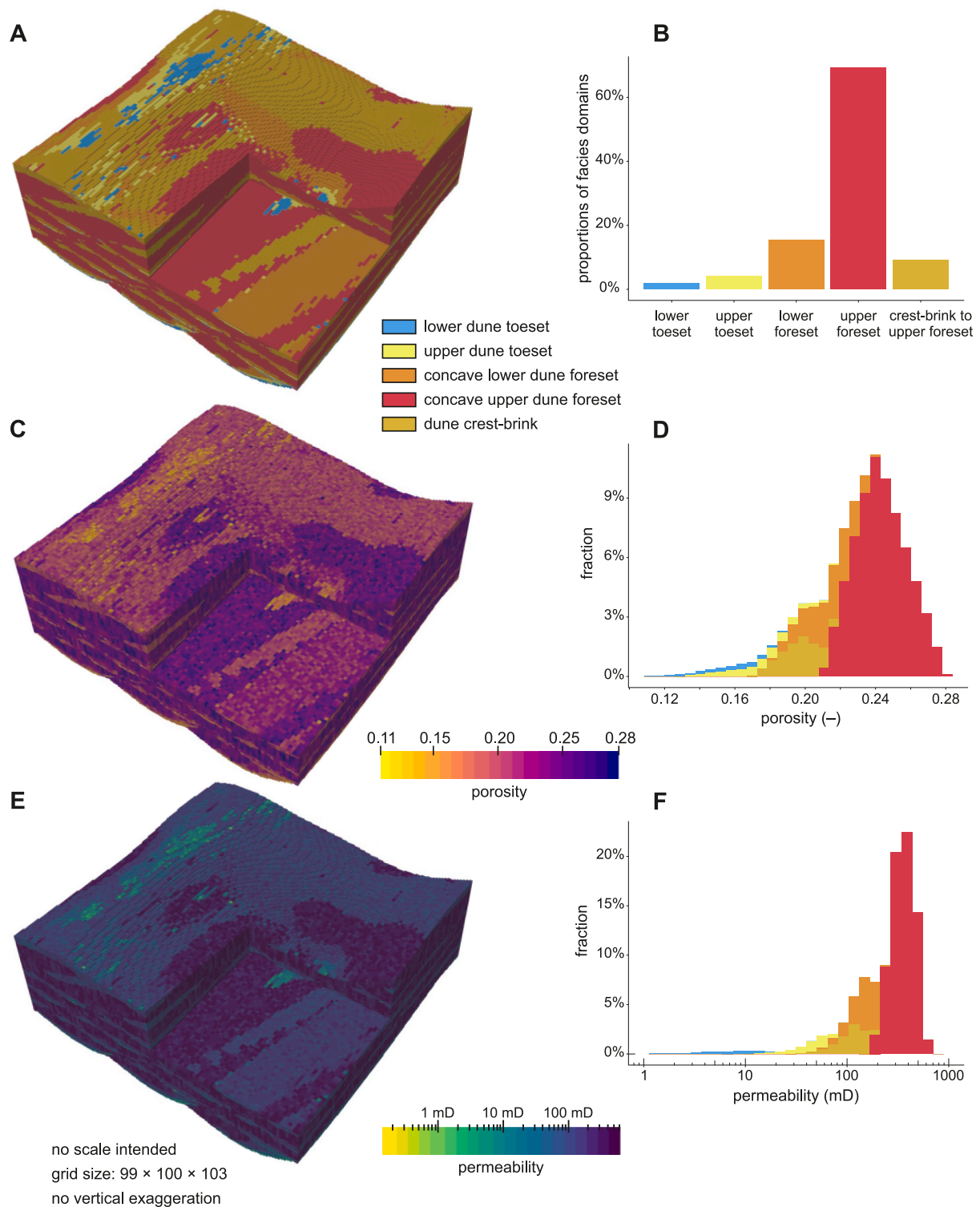
Fig. 9. Outputs of static geocellular modelling aided by DASH, for a succession related to superimposed dunes. (A) Geocellular model of DASH facies domains, with their proportions charted in (B). Facies-domain proportions reflect in part the full preservation of modelled bedforms on the top surface: the proportion of crest-brink to upper foreset domain volumes is ca. 5% in the part of grid underlying the top surface, as opposed to ca. 9% in the entire grid. (C) Realization of a Sequential Gaussian Simulation of porosity values modelled in the facies domains shown in (A); distributions of porosity values vary across the facies domains as shown in (D). (E) Realization of a Sequential Gaussian Simulation of permeability values modelled in the facies domains shown in (A); distributions of porosity values vary across the facies domains as shown in (F). Note that in the majority of ancient successions, the original dune topography and the facies associated with it are not preserved.

4. Example model outputs

Examples of the stratigraphic architectures arising from the migration of aeolian dunes of different morphology and with varying complexity are presented to demonstrate how the DASH model can generate facies distributions and heterogeneity that match closely with examples observed in nature. The facies domains incorporated in the model outputs are also used to produce static geocellular models
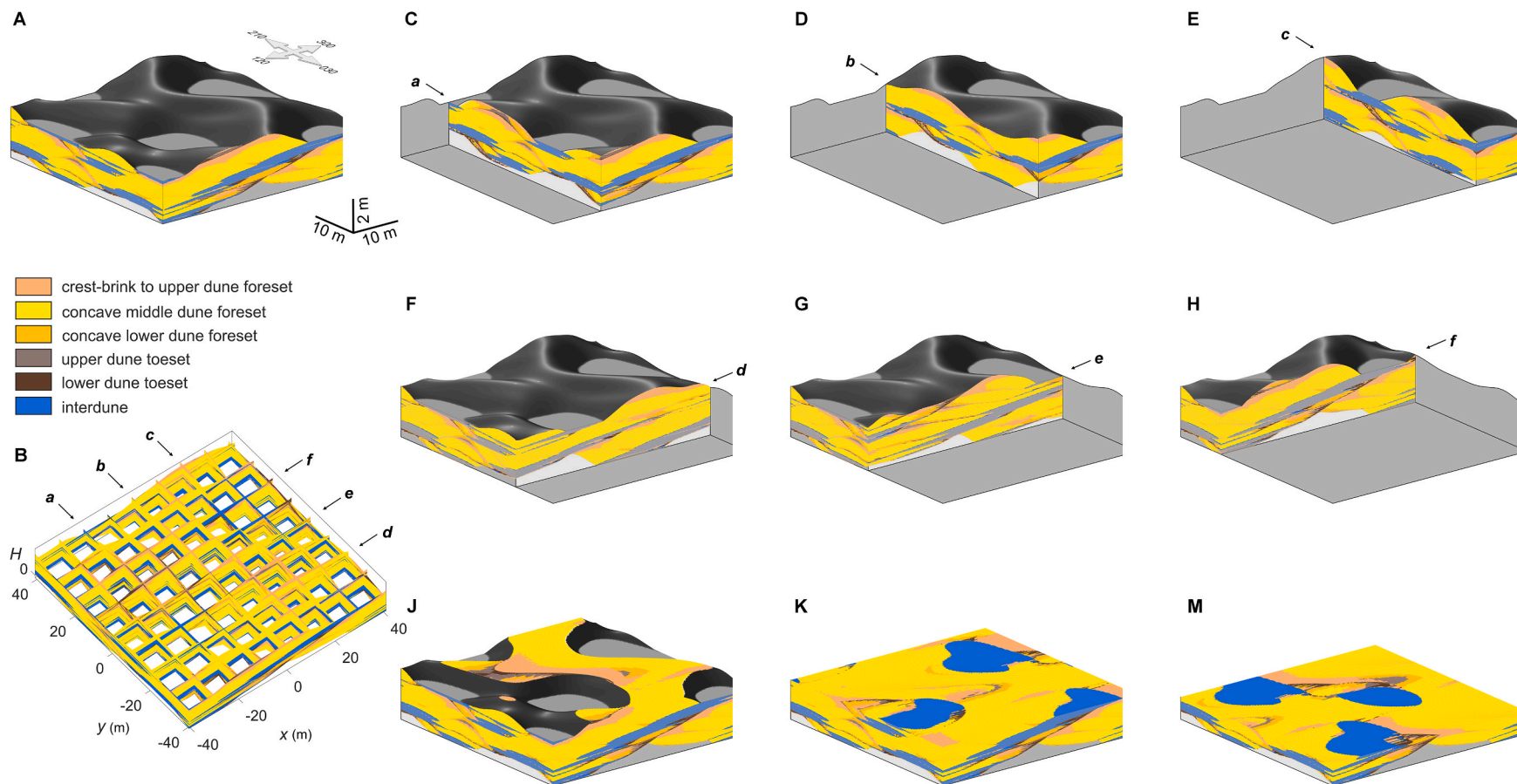
Fig. 10. Three-dimensional geomorphology and sedimentary architecture and lithofacies distributions of a succession that embodies the architecture and facies distribution of the Triassic Helsby Sandstone Formation, Cheshire Basin, UK (Mountney and Thompson, 2002). Default facies types, as defined in DASH, are used.

depicting spatial variations in porosity and permeability fields. Because the preservation of the formative surface topography has an impact on proportions of facies domains, the output grids generated from DASH are usually truncated in their upper parts to mimic subsequent erosion so as to obtain facies-domain proportions that consider sediment preservation realistically. The way in which the facies domains may reflect the spatial distribution of facies with contrasting petrophysical properties has been considered by applying the model output as a geocellular grid with regions in which petrophysical properties can be modelled stochastically. Values of porosity and permeability are modelled in the different domains using the Sequential Gaussian Simulation (SGS) algorithm in SGeMS (Remy et al., 2009). SGS is constrained using the following approaches: (i) distributions in petrophysical properties that reflect both the relative proportion of different facies types (grainflow, grainfall and wind-ripple strata) in the facies domains and values of porosity and permeability that are typical for these facies types, established on the basis of a synthesis of literature data (Besly et al., 2018; Ringrose and Bentley, 2016; Tillman and Coalson, 1989); and (ii) a variogram model with range values smaller than the grid cell size. The choice of small variogram ranges has been made to illustrate how this approach to static-model building generates spatial distributions in porosity and permeability that primarily reflect the geometry of the facies domains. The different examples are compared in terms of the proportions and geometries of the facies domains, and of the distributions and spatial variability in the petrophysical properties. The generated models can be used to examine stratigraphic complexity of aeolian deposits in 3D and to assist in subsurface characterization.

4.1. Idealized example: transverse dunes

This idealized example aims to model the architecture produced by the migration of three-dimensional, invariable transverse dunes climbing at a low (subcritical) angle. The internal architecture is illustrated in terms of (i) bounding surfaces of different orders and (ii) facies domains that are coded according to the default classes described above. The model uses the same parameter settings as for case 34a by Rubin and Carter (2006). The generated sedimentary architecture and facies distributions are shown in Fig. 4. Transverse dunes migrate under the influence of a net unimodal wind direction. The dune crestlines are out of phase and extended perpendicular to the dune migration direction. Dune migration and aggradation generate trough cross-bedding in which trough widths are controlled by the wavelength of along-crest sinuosity. Dune crest-brink to upper foreset regions are thickest at the trough centre and thin out towards the edges (Fig. 4A&B). Concave dune foresets are preserved at the trough sides where slopes are relatively steep. Dune toesets are preserved at the very bottom of the trough or at the edge of enclosed lozenge-shaped packages seen in the horizontal sections (Fig. 4G&K). In this theoretical modelled example, facies proportions are determined in part by an exceptionally high rate of aggradation relative to bedform celerity, as indicated by an angle of climb equal to 5°. The frequency distributions in values of porosity and permeability across the geocellular grid are notably bimodal, which reflects the dominance of upper and middle foreset domains under the imposed conditions of rapid aggradation (Fig. 5).

4.2. Idealized example: longitudinal dunes

This idealized example aims to model the architecture produced by the morphodynamic evolution of longitudinal (linear) dunes. Model outputs, presented in Fig. 6, are obtained using the default classes of facies domains (see above) and the parameter settings of case 55 by Rubin and Carter (2006). The sinuous crests of the longitudinal dunes extend along the direction of dune migration. Longitudinal dunes tend to develop under two dominant converging wind directions oriented obliquely to the crests. As a result, the preserved facies domains are elongated along the trend of the crestlines. Dune crest-brink to upper

foreset regions are extended along the ridges, whereas dune-toeset facies domains occupy interdune corridors. This example mimics special conditions in which dunes accrete vertically without net lateral migration (Bagnold, 1941). Tsoar (1982) documented dunes whose evolution produced a similar sedimentary architecture in the Sinai Desert. Steele (1983) also interpreted a similar style of longitudinal dunes preserved in the Permian Yellow Sands of Northeast England. In reality, longitudinal dunes are commonly characterized by some component of lateral mobility, and their accumulated deposits tend to be characterized by cross strata with a relatively unimodal dip directions resembling those produced by transverse dunes (Besly et al., 2018; Bristow et al., 2000; Rubin and Hunter, 1985). However, in this theoretical case example, no such component of lateral creep is incorporated. Relative to the example for transverse dunes presented above, the results of geostatistical modelling highlight markedly different spatial distributions in porosity and permeability in the geocellular grid. The modelled petrophysical properties and their variation across the grid reflect the different proportions and geometries of the preserved facies domains (Fig. 7). Frequency distributions of petrophysical properties are multimodal, and reflect primarily the enhanced preservation of dune-toeset domains associated with conditions of relatively laterally stable linear dunes.

4.3. Idealized example: superimposed dunes

This idealized example aims to model the architecture produced by the migration of superimposed bedforms with along-crest dune migration, modelled using the same parameter settings of case 46l by Rubin and Carter (2006). The resulting internal architecture is shown in Fig. 8, which highlights the presence of topographic depressions resembling scour pits formed by the intersection of troughs of the two sets of bedforms. The superimposed bedforms migrate transverse to the motion of the main (parent) bedform. This leads to the scour pits to migrate obliquely to the crestlines of the main bedforms, as can be recognized in the horizontal sections (Fig. 8K). Dune forests are dominant on slopes, and dune toesets are preserved as a thin layer restricted along the bottom of troughs. Relative to the examples shown above, the spatial distributions in porosity and permeability in the geocellular grid are more complex, highlighting the control exerted by complex morphodynamic behaviours in controlling the preservation of different physiographic domains with contrasting facies make-ups (Fig. 9).

4.4. A real-world example: the Triassic Helsby Sandstone Formation, Cheshire Basin, UK

The Triassic Helsby Sandstone Formation is a well-exposed mixed aeolian-fluvial succession. Mountney and Thompson (2002) couple extensive and detailed architectural element data with foreset and bounding surface dip and azimuth data, and use the numerical model by Rubin and Carter (2006) to quantitatively reconstruct the three-dimensional geometry of the aeolian and interdune deposits. Mountney and Thompson (2002) demonstrate how variably damp or wet interdune deposits can be preserved in a variety of geometries depending on the rates of dune migration, sediment supply, and shifts in water table, else in relation to fluvial flooding (cf. Carr-Crabaugh and Kocurek, 1998; Crabaugh and Kocurek, 1993). However, numerical modelling results by Mountney and Thompson (2002) only demonstrate stratal geometries in the form of architectural elements and their bounding surfaces of different orders, without explicitly presenting the associated facies distributions.

Here, the input parameters to DASH are the same as those employed by Mountney and Thompson (2002). DASH is applied to recreate the expected 3D distribution of facies that matches with observations from the Frogsmouth unit of the Triassic Helsby Sandstone Formation; the use of these same inputs in DASH enables the generation of models that incorporate both stratal architectures and facies distributions in three dimensions (Fig. 10). The modelling output shows the curved (sinuous)
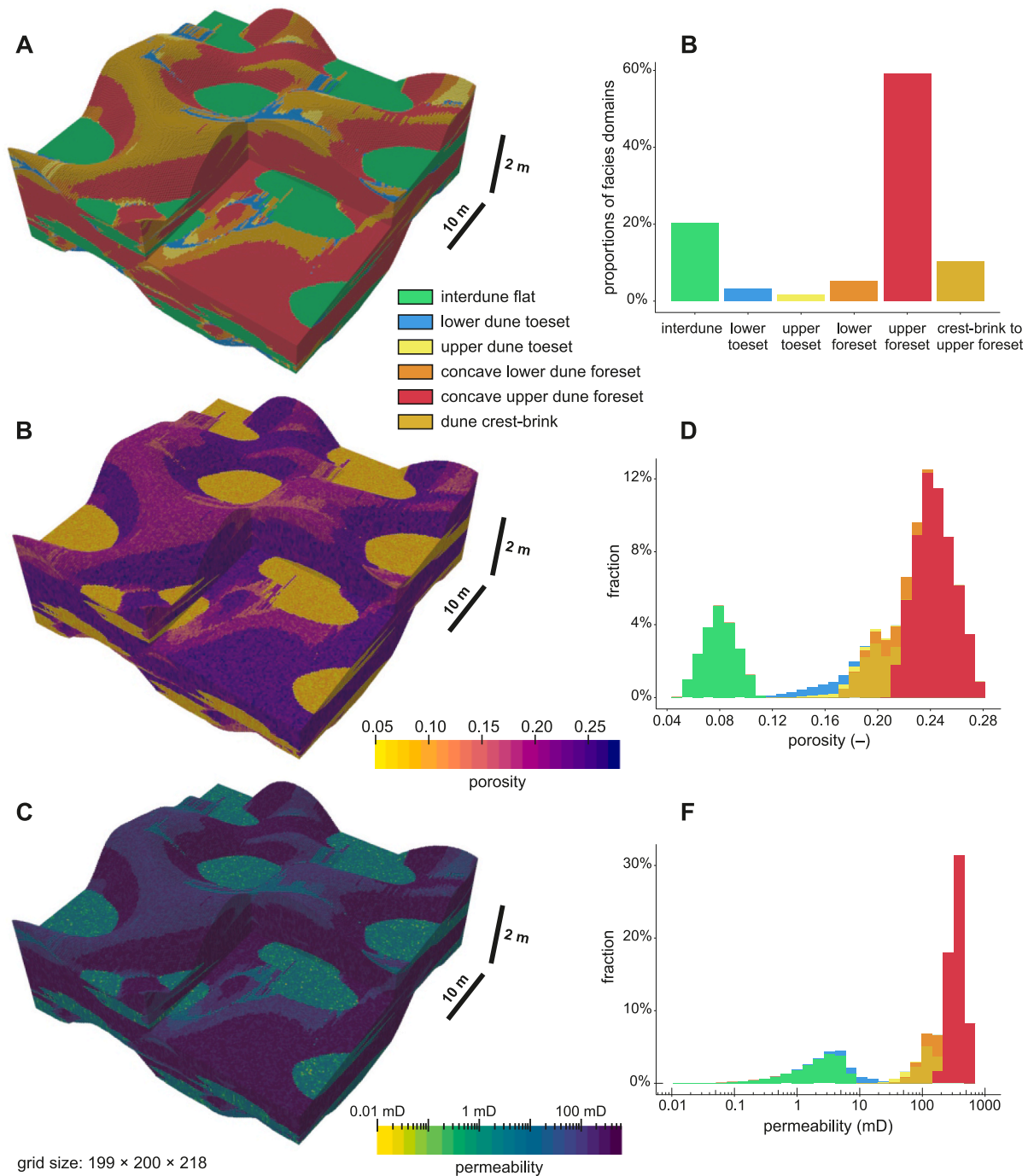
Fig. 11. Outputs of static geocellular modelling aided by DASH, for a succession that embodies the stratal architecture of the Helsby Sandstone Formation. (A) Geocellular model of DASH facies domains, with their proportions charted in (B). Facies-domain proportions reflect in part the full preservation of modelled bedforms on the top surface: the proportion of crest-brink to upper foreset and interdune domains are ca. 5% and 26% in the part of grid underlying the top surface, as opposed to ca. 10% and 20%, respectively, in the entire grid. (C) Realization of a Sequential Gaussian Simulation of porosity values modelled in the facies domains shown in (A); distributions of porosity values vary across the facies domains as shown in (D). (E) Realization of a Sequential Gaussian Simulation of permeability values modelled in the facies domains shown in (A); distributions of porosity values vary across the facies domains as shown in (F). Note that in the preserved Triassic Helsby Sandstone Formation, the original dune topography and the facies associated with it are not preserved. Here we reconstruct the original dune morphology and its associated facies distribution for the purpose of interpreting the palaeoenvironment of deposition.

crests of the original primary bedforms and out-of-phase superimposed bedforms migrating obliquely over the parent forms. Consequently, interdune areas form depressions that are commonly spatially isolated in planform (Fig. 10A). However, preserved damp- or wet-interdune deposits can, in places, extend continuously, as revealed in cross sections (Fig. 10C&K). The angle of climb for the bedforms is approximately 1.5°, which is within the range of angles of climb measured directly from

stratal relationships by Mountney and Thompson (2002). Preserved deposits are dominated by concave-up middle dune forests. Dune crest-brink and upper foreset deposits are partially preserved and towards one side of troughs due to the oblique component of original bedform migration (Fig. 10D). Dune toesets are solely restricted to the very bottom of dune cross strata (Fig. 10K&M).

Compared to the idealized examples described above, in this case,

the outputs of geostatistical petrophysical modelling (Fig. 11) are characterized by: (i) larger variability in both porosity and permeability values, largely due to the preservation of interdune domains; (i) increased complexity in the spatial distributions of domains with contrasting petrophysical properties; the effect imparted by the presence of interdune deposits on the tortuosity of higher reservoir quality units is notable.

5. Summary and conclusions

In the subsurface, aeolian sedimentary successions form important hydrocarbon reservoirs, potable aquifers, geothermal reservoirs, sites for hydrogen storage, and repositories for carbon capture, utilization and storage (CCUS), as is the case for the Triassic aeolian deposits in the Cheshire Basin of England (Hirst et al., 2015), for example. It is therefore necessary to develop tools that can be employed to generate quantitative descriptions of subsurface aeolian architectures that are geologically realistic. The DASH model addresses this need. DASH serves different purposes, and can be used for different geological applications: (i) to help visualize, in 3D, both the stratal architecture and the lithological heterogeneity of sedimentary architectures that are thought to be present in the subsurface based on limited borehole or geophysical data; (ii) to generate training images that capture patterns of geological heterogeneity and that can be used as input to Multiple-Point Statistics (MPS) modelling tools (e.g., SNESIM, DS, FILTERSIM; Mariethoz et al., 2010; Strebelle, 2002; Wu et al., 2008) in geocellular modelling (cf. Montero et al., 2021); a large number (in the order of 10^4) of unconditional MPS facies models that are based on training images obtained from DASH may in turn be applied as training dataset with which to constrain geocellular modelling methods based on machine learning, such as approaches that use generative adversarial networks (cf. Chan and Elsheikh, 2019; Zhang et al., 2019); (iii) to assist flow-based upscaling of petrophysical properties in conjunction with other tools providing descriptions of lamina and lamina-set heterogeneity; this way, static property models embodying realistic distributions of petrophysical properties can be created (Nordahl et al., 2014); (iv) to explore how different autogenic and allogenic factors control the nature of the preserved aeolian sedimentary record and their impacts on the static connectivity of facies domains resulting in pathways of fluid flow and solute transport (cf. Hovadik and Larue, 2007; Colombera and Mountney, 2021); and (v) to guide interpretations of the rock record, by (i) providing facies models to be used as references for comparison with facies architectures seen in outcrop, and by (ii) elucidating the effects of dune morphodynamics and erg evolution on facies preservation. A key limitation of the DASH model lies in its simplified modelling approach, which is based on inferred attributes of formative geomorphic features and geological understanding of facies organization of aeolian successions; it therefore disregards flow dynamics, sediment-transport processes and dune-field morphodynamics (cf. Parteli, 2022). Nonetheless, the DASH model serves as a powerful tool that allows exploration of 3D sedimentary architecture and preserved facies distribution in aeolian successions in a computationally effective way, and without requiring knowledge of variables defining physical processes.

6. Code availability section

Name of the code/library: DASH.
Contact: n.yan@leeds.ac.uk.
Program language: MATLAB.
The source code and case examples are available for downloading from Yan N. (2023) DASH_v1.0 source code. University of Leeds. [Dataset] https://doi.org/10.5518/1448.

CRediT authorship contribution statement

Na Yan: Conceptualization, Data curation, Formal analysis,

Methodology, Software, Visualization, Writing – original draft, Writing – review & editing. **Luca Colombera:** Conceptualization, Data curation, Formal analysis, Methodology, Visualization, Writing – original draft, Writing – review & editing. **Grace I.E. Cosgrove:** Methodology, Writing – original draft, Writing – review & editing. **Nigel P. Mountney:** Conceptualization, Data curation, Methodology, Writing – original draft, Writing – review & editing.

Declaration of competing interest

The authors declare that they have no known competing financial interests or personal relationships that could have appeared to influence the work reported in this article.

Data availability

Data will be made available on request. The source code and case examples are available for downloading from Yan N. (2023) DASH_v1.0 source code. University of Leeds. [Dataset] https://doi.org/10.5518/1448.

References

Al-Masrahy, M., 2020. Significance of Aeolian Deposits Resultant Drift Direction, Implications for Reservoir Prediction, Utilizing Subsurface and Analogue Data. International Petroleum Technology Conference.

Al-Masrahy, M.A., Mountney, N.P., 2013. Remote sensing of spatial variability in aeolian dune and interdune morphology in the Rub'Al-Khali, Saudi Arabia. Aeolian Res 11, 155–170.

Bagnold, R.A., 1941. The Physics of Blown Sand and Desert Dunes. Methuen & Co. Ltd, London.

Besly, B., Romain, H.G., Mountney, N.P., 2018. Reconstruction of linear dunes from ancient aeolian successions using subsurface data: Permian Auk Formation, Central North Sea, UK. Mar. Petrol. Geol. 91, 1–18.

Bristow, C.S., Bailey, S., Lancaster, N., 2000. The sedimentary structure of linear sand dunes. Nature 406, 56–59.

Carr-Crabaugh, M., Kocurek, G., 1998. Continental sequence stratigraphy of a wet eolian system: a key to relative sea level change. In: Shanley, K.W., McCabe, P.J. (Eds.), Relative Role of Eustasy, Climate, and Tectonism in Continental Rocks, vol. 59. SEPM Special Publication, pp. 213–228.

Chan, S., Elsheikh, A.H., 2019. Parametric generation of conditional geological realizations using generative neural networks. Comput. Geosci. 23, 925–952.

Colombera, L., Mountney, N.P., 2021. Influence of fluvial crevasse-splay deposits on sandbody connectivity: lessons from geological analogues and stochastic modelling. Mar. Petrol. Geol. 128, 105060.

Colombera, L., Yan, N., McCormick-Cox, T., Mountney, N.P., 2018. Seismic-driven geocellular modeling of fluvial meander-belt reservoirs using a rule-based method. Mar. Petrol. Geol. 93, 553–569.

Cosgrove, G.I.E., Colombera, L., Mountney, N.P., 2021. A database of Aeolian Sedimentary Architecture for the characterization of modern and ancient sedimentary systems. Mar. Petrol. Geol. 127, 104983.

Crabaugh, M., Kocurek, G., 1993. Entrada Sandstone: an Example of a Wet Aeolian System, vol. 72. Geological Society, London, Special Publications, pp. 103–126.

Deutsch, C.V., Journel, A.G., 1992. Geostatistical software library and user's guide. N. Y. 119, 578.

Fryberger, S.G., 1979. Dune forms and wind regime. In: McKee, E.D. (Ed.), A Study of Global Sand Seas. US Geological Survey Professional Paper, Washington, pp. 137–169.

Gross, E.C., Carr, M., Jobe, Z.R., 2023. Three-dimensional bounding surface architecture and lateral facies heterogeneity of a wet aeolian system: entrada Sandstone, Utah. Sedimentology 70, 145–178.

García-Hidalgo, J.F., Temiño, J., Segura, M., 2002. Holocene eolian sediments on the southern border of the Duero Basin (Spain): origin and development of an eolian system in a temperate zone. J. Sediment. Res. 72, 30–39.

Glennie, K., Provan, D., 1990. Lower permian rotliegend reservoir of the southern North sea gas province. In: Brooks, J. (Ed.), Classic Petroleum Provinces, vol. 50. Geological Society Special Publications, pp. 399–416.

Hirst, C.M., Gluyas, J.G., Adams, C.A., Mathias, S.A., Bains, S., Styles, P., 2015. UK low enthalpy geothermal resources: the Cheshire Basin. In: Proceedings of the World Geothermal Congress, pp. 19–25.

Hovadik, J.M., Larue, D.K., 2007. Static characterizations of reservoirs: refining the concepts of connectivity and continuity. Petrol. Geosci. 13, 195–211.

Hunter, R.E., 1977. Basic types of stratification in small eolian dunes. Sedimentology 24, 361–387.

Inman, D., Ewing, G., Corliss, J., 1966. Coastal sand dunes of guerrero negro, baja California, Mexico. Geol. Soc. Am. Bull. 77, 787–802.

Journel, A.G., Xu, W., 1994. Posterior identification of histograms conditional to local data. Math. Geol. 26, 323–359.

Kocurek, G., 1981. Significance of interdune deposits and bounding surfaces in aeolian dune sands. Sedimentology 28, 753–780.

Kocurek, G., Dott, R.H., 1981. Distinctions and uses of stratification types in the interpretation of eolian sand. J. Sediment. Res. 51, 579–595.

Kocurek, G., Goudie, A., Livingstone, I., Stokes, S., 1999. The aeolian rock record (Yes, Virginia, it exists, but it really is rather special to create one). In: Goudie, A.S., Livingstone, I., Stokes, S. (Eds.), Aeolian Environments, Sediments and Landforms. John Wiley & Sons, Ltd, Chichester, pp. 239–259.

Kocurek, G., Havholm, K., 1993. Eolian sequence stratigraphy-a conceptual framework. In: Eimer, P., Posamentier, H. (Eds.), Siliciclastic Sequence Stratigraphy, vol. 58. AAPG Memoir, pp. 393–409.

Kocurek, G., Knight, J., Havholm, K., 1991. Outcrop and semi-regional three-dimensional architecture and reconstruction of a portion of the eolian Page Sandstone (Jurassic). In: Miall, A.D., Tyler, N. (Eds.), The Three-Dimensional Facies Architecture of Terrigenous Clastic Sediments and its Implications for Hydrocarbon Discovery and Recovery. SEPM Concepts in Sedimentology and Paleontology, pp. 25–43.

Lancaster, N., 1997. Response of eolian geomorphic systems to minor climate change: examples from the southern Californian deserts. Geomorphology 19, 333–347.

Lindquist, S.J., 1988. Practical characterization of eolian reservoirs for development: nugget Sandstone, Utah—Wyoming thrust belt. Sediment. Geol. 56, 315–339.

Luthi, S.M., Banavar, J.R., 1988. Application of borehole images to three-dimensional geometric modeling of eolian sandstone reservoirs, Permian Rotliegende, North Sea. AAPG (Am. Assoc. Pet. Geol.) Bull. 72, 1074–1089.

Mariethoz, G., Renard, P., Straubhaar, J., 2010. The direct sampling method to perform multiple-point geostatistical simulations. Water Resour. Res. 46, W11536.

McKee, E.D., 1966. Structures of dunes at white sands national monument, New Mexico (and a comparison with structures of dunes from other selected areas). Sedimentology 7, 3–69.

McKee, E.D., Bigarella, J.J., 1979. Sedimentary structures in dunes. In: McKee, E.D. (Ed.), A Study of Global Sand Seas, vol. 1052. U.S. Geological Survey Professional Paper, pp. 83–134.

Montero, J.M., Colombera, L., Yan, N., Mountney, N.P., 2021. A workflow for modelling fluvial meander-belt successions: combining forward stratigraphic modelling and multi-point geostatistics. J. Petrol. Sci. Eng., 108411

Mountney, N., Russell, A., 2006. Coastal aeolian dune development, Sólheimasandur, southern Iceland. Sediment. Geol. 192, 167–181.

Mountney, N.P., 2006. Eolian facies models. In: Posamentier, H.W., Walker, R.G. (Eds.), Facies Models Revisited. SEPM Society for Sedimentary Geology, pp. 19–83.

Mountney, N.P., 2012. A stratigraphic model to account for complexity in aeolian dune and interdune successions. Sedimentology 59, 964–989.

Mountney, N.P., Thompson, D.B., 2002. Stratigraphic evolution and preservation of aeolian dune and damp/wet interdune strata: an example from the Triassic Helsby Sandstone Formation, Cheshire Basin, UK. Sedimentology 49, 805–833.

Mullins, J., Pierce, C., Rieke, H., Howell, J., 2022. Aeolian sand dune sedimentary architecture is key in determining the "slow-gas effect" during gas field production performance. SPE J. 27, 1354–1366.

Nordahl, K., Messina, C., Berland, H., Rustad, A.B., Rimstad, E., 2014. Impact of multiscale modelling on predicted porosity and permeability distributions in the fluvial deposits of the Upper Lunde Member (Snorre Field, Norwegian Continental Shelf). In: Martinius, A.W., Howell, J.A., Good, T.R. (Eds.), Sediment-Body Geometry and Heterogeneity: Analogue Studies for Modelling the Subsurface, vol. 387. Geological Society, London, Special Publications, pp. 85–109.

North, C.P., Boering, M., 1999. Spectral gamma-ray logging for facies discrimination in mixed fluvial-eolian successions: a cautionary tale. AAPG (Am. Assoc. Pet. Geol.) Bull. 83, 155–169.

Parteli, E.J.R., 2022. Physics and modeling of wind-blown sand landscapes. In: Shroder, J.J.F. (Ed.), Treatise on Geomorphology, second ed. Elsevier, Academic Press, pp. 20–52.

Reading, H.G., 2009. Sedimentary Environments: Processes, Facies and Stratigraphy. John Wiley & Sons.

Remy, N., Boucher, A., Wu, J., 2009. Applied Geostatistics with SGeMS: A User's Guide. Cambridge University Press, Cambridge.

Ringrose, P., Bentley, M., 2016. Reservoir Model Design. Springer.

Rodríguez-López, J.P., Clemmensen, L.B., Lancaster, N., Mountney, N.P., Veiga, G.D., 2014. Archean to Recent aeolian sand systems and their sedimentary record: current understanding and future prospects. Sedimentology 61, 1487–1534.

Romain, H.G., 2014. Controls on Aeolian Bed-Set Architecture and Implications for Reservoir Heterogeneity. University of Leeds.

Romain, H.G., Mountney, N.P., 2014. Reconstruction of three-dimensional eolian dune architecture from one-dimensional core data through adoption of analog data from outcrop. AAPG (Am. Assoc. Pet. Geol.) Bull. 98, 1–22.

Rubin, D.M., 1987. Cross-Bedding, Bedforms, and Paleocurrents. Society of Economic Paleontologists and Mineralogists, Tulsa.

Rubin and Carter, 2005. https://pubs.usgs.gov/of/2005/1272/.

Rubin, D.M., Carter, C.L., 2006. Cross-bedding, Bedforms, and Paleocurrents. Society for Sedimentary Geology.

Rubin, D.M., Hunter, R.E., 1985. Why deposits of longitudinal dunes are rarely recognized in the geologic record. Sedimentology 32, 147–157.

Steele, R.P., 1983. Longitudinal draa in the permian Yellow sands of North-Fast England. In: Brookfield, M.E., Ahlbrandt, T.S. (Eds.), Developments in Sedimentology. Elsevier, pp. 543–550.

Strebelle, S., 2002. Conditional simulation of complex geological structures using multiple-point statistics. Math. Geol. 34, 1–21.

Tillman, L.E., Coalson, E., 1989. Sedimentary facies and reservoir characteristics of the nugget sandstone (Jurassic), painter reservoir field, uinta county, Wyoming. In: Coalson, E.B., Kaplan, S.S. (Eds.), Petrogenesis and Petrophysics of Selected Sandstone Reservoir of the Rocky Mountain Region. Rocky Mountain Association of Geologists, pp. 97–108.

Tsoar, H., 1982. Internal structure and surface geometry of longitudinal (seif) dunes. J. Sediment. Res. 52, 823–831.

Wasson, R.J., Hyde, R., 1983. Factors determining desert dune type. Nature 304, 337–339.

Wu, J., Boucher, A., Zhang, T., 2008. A SGeMS code for pattern simulation of continuous and categorical variables: FILTERSIM. Comput. Geosci. 34, 1863–1876.

Yaalon, D., Laronne, J., 1971. Internal structures in eolianites and paleowinds, Mediterranean coast, Israel. J. Sediment. Res. 41, 1059–1064.

Yan, N., Baas, A.C.W., 2015. Parabolic dunes and their transformations under environmental and climatic changes: towards a conceptual framework for understanding and prediction. Global Planet. Change 124, 123–148.

Zhang, T.-F., Tilke, P., Dupont, E., Zhu, L.C., Liang, L., Bailey, W., 2019. Generating geologically realistic 3D reservoir facies models using deep learning of sedimentary architecture with generative adversarial networks. Petrol. Sci. 16, 541–549.